Absorption and scattering imaging of tissue with steady-state second-differential spectral-analysis tomography

Heng Xu, Brian W. Pogue, Hamid Dehghani, and Keith D. Paulsen

Thayer School of Engineering, Dartmouth College, Hanover, New Hampshire 03755

Roger Springett and Jeff F. Dunn

Department of Diagnostic Radiology, Dartmouth Medical School, Hanover, New Hampshire 03755

Received May 17, 2004

A novel approach to reconstructing both the absorption and the scattering properties of a turbid medium simultaneously from steady-state broadband spectral measurements is presented that utilizes second-differential fitting to the water spectrum to estimate the optical path length in tissue. Theoretical and experimental evidence is provided to demonstrate the robust accuracy of the spectroscopy approach and reconstructed absorption images. The steady-state broadband CCD system has the potential to provide accurate chromophore imaging without the technological complexity of time- or frequency-domain systems. © 2004 Optical Society of America

OCIS codes: 170.0110, 170.3880, 170.6960, 170.6510.

Near-infrared (NIR) imaging has become a promising modality for the study of human tissue because it has the ability to qualify hemoglobin content and oxygenation in spatially resolved images. The major limitation of NIR imaging has always been related to the fact that light experiences many scattering events when passing through tissue, and the collected optical signal is a nonlinear function of both the absorption and the scattering properties of the medium. To fulfill the advantage of NIR imaging, the most challenging problem is to separate absorption and scattering properties, thereby allowing interpretation of the chromophore concentration by use of linear absorbance spectroscopy. In this Letter we report a novel method of reconstructing both absorption and reduced scattering properties in a turbid medium from steady-state boundary data by applying the principles of second-differential spectroscopy to an imaging problem. Here our boundary data are measured by a broadband steady-state full spectral CCD system, and the term steady state is used to distinguish the system from the conventional boundary data type provided by time-domain systems (TDSs) or frequency-domain systems (FDSs).

In the NIR range the diffusion approximation of transport is widely accepted as a practical model in which the distribution of the optical properties within the domain can be determined from measurements of the light distribution through the tissue surface. The uniqueness of this determination has been investigated,[1] and the conclusion has been widely accepted that the solution is not unique when single-wavelength steady-state diffusion-based measurements are used, resulting in an inability to separate local absorption from local scattering values. Recent studies demonstrated that the use of multiple wavelengths in image reconstruction, along with *a priori* estimates of the spectral features, can potentially solve the problems of having a nonunique solution[2,3] through a constraint-based implementation in the image reconstruction process. The uniqueness needs to be taken into context with TDS or FDS systems, which are thought to provide a secondary independent measurement that is more uniquely associated with the scattering coefficient, thereby providing a reliable method of separating these coefficients. Although the actual image reconstruction is an inevitably ill-posed problem because of limitations in the experimental setup and the numerical approach, least-squares iterative optimization algorithms have shown successful recovery of both absorption and scattering properties.[4] In this Letter a proposed method is reported that relies on broadband spectroscopy but also provides a direct measurement of the optical path length, thereby providing a more robust data set for quantification of chromophore concentrations. This approach can be explained by the fact that the differential path length (DP) can consequently be derived from the broadband attenuation spectrum by use of our second-differential spectral analysis (SDSA) method and provides another constraint to solve the inverse problem uniquely, given additional input information about the water concentration of the tissue. Since physically the DP is an equivalent measure of mean optical path length to that of mean flight time by TDS or phase shift by FDS,[5] our approach is essentially consistent with the other two methods.

A diagram of the broadband steady-state CCD-based system is shown in Fig. 1. The light source is a dc-regulated broadband quartz halogen lamp filtered to generate the NIR source (650–950 nm). The source locations are turned on sequentially and attenuated through the object and collected simultaneously by eight receiver fibers. The detected signals are horizontally dispersed through a grating in the spectrograph, and the resulting spectra are integrated simultaneously in the CCD camera. The quantitative measurement set from the tissue is the attenuation spectrum between all source and detector pairs.

The DP is defined as the ratio of the differential attenuation to the absorption ($\partial A/\partial \mu_a$). The method of SDSA was first introduced by Matcher *et al.*,[6] and a

0146-9592/04/172043-03$15.00/0

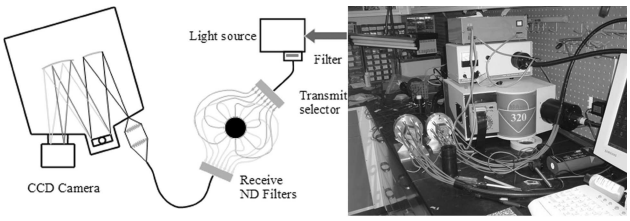

Fig. 1. Left, Diagram of the multichannel broadband full-spectral CCD system. Right, photograph of the system with the filter wheels and the source wheel at the left and the source and the spectrometer at the right.

more rigorous derivation was discussed in our previous paper.[7] The attenuation (A) is determined by the absorption (μ_a) and reduced scattering (μ_s') properties, which are wavelength dependent, so the second derivative of attenuation with respect to wavelength (λ) can be expanded as

$$\frac{\mathrm{d}^2A}{\mathrm{d}\lambda^2} = \frac{\partial A}{\partial \mu_a}\frac{\mathrm{d}^2\mu_a}{\mathrm{d}\lambda^2} + \frac{\partial A}{\partial \mu_s'}\frac{\mathrm{d}^2\mu_s'}{\mathrm{d}\lambda^2} + \frac{\mathrm{d}(\partial A/\partial \mu_a)}{\mathrm{d}\lambda}\frac{\mathrm{d}\mu_a}{\partial \lambda} + \frac{\mathrm{d}(\partial A/\partial \mu_s')}{\mathrm{d}\lambda}\frac{\mathrm{d}\mu_s'}{\partial \lambda}. \quad (1)$$

It has been found that, with the chromophores present in tissue with a weak wavelength dependence of the scattering coefficient of the tissue, the last three terms are small compared with the first term. Therefore, it is reasonable to make the approximation that

$$\frac{\mathrm{d}^2A}{\mathrm{d}\lambda^2} \approx \frac{\partial A}{\partial \mu_a}\frac{\mathrm{d}^2\mu_a}{\mathrm{d}\lambda^2}. \quad (2)$$

Given that the absorption coefficient is a linear summation of the concentration of the chromophores (C_i) multiplied by their known extinction coefficients (ϵ_i) and $\mathrm{d}A/\mathrm{d}\mu_a$ is replaced by DP, Eq. (2) can be further expanded as

$$\frac{\mathrm{d}^2A}{\mathrm{d}\lambda^2} = \sum_{i=1}^{N_c}\left(\mathrm{DP}\,C_i\frac{\mathrm{d}^2\epsilon_i}{\mathrm{d}\lambda^2}\right), \quad (3)$$

where N_c is the number of chromophores. In reality, $\mathrm{d}^2\epsilon_i/\mathrm{d}\lambda^2$ are some peaks in some narrow wavelength ranges, whereas DP exhibits weak wavelength dependence; therefore, it is possible to use the zero-order approximation of DP in such a narrow range. Since $\mathrm{d}^2A/\mathrm{d}\lambda^2$ is the measured response and the right side of Eq. (3) can be regarded as the linear summation of the chromophores' absorption feature ($\mathrm{d}^2\epsilon_i/\mathrm{d}\lambda^2$), when λ is discretized in a narrow range, Eq. (3) is a solvable overdetermined linear problem. Hence the coefficients ($\mathrm{DP}\,C_i$) can be calculated by use of multilinear regression. Since water has prominent absorption features near 740 and 840 nm, the DP at these features can be calculated by taking the water concentration into account. In practice, because of the presence of noise and cross talk between chromophores, a broader wavelength range is typically chosen to get better fitting results. The fitting ranges are empirically chosen as 700–800 nm for 740 nm and 800–880 nm for 840 nm. Indeed, besides the DP information, SDSA also provides a means to estimate the concentration of other chromophores that have significant features in the second-differential spectrum. The one-dimensional analysis we made above can be extended into multiple dimensions by integrating the DP over the imaging domain.

Clearly, when the SDSA method is applied, several assumptions and approximations are made. It is thus interesting to investigate whether the calculated DP from the SDSA method has good agreement with the actual DP and whether absorption and reduced scattering properties can be successfully recovered with this calculated DP and the measured attenuation. To look into this question we completed a series of simulations. The attenuation spectra were generated by the diffusion-approximation-based forward model. The DP was calculated by application of the SDSA method to the noise-added attenuation spectra data, and the actual DP was calculated by the forward model as well. The agreement of the calculated and the actual DP was examined in various situations. The details can be found in Ref. 7. In most cases the difference was within a few percent and was insensitive to position, chromophore composition, or the scattering coefficient of the medium as long as the water was distributed homogeneously within the medium. If water is inhomogeneously distributed, a water map [acquired by magnetic resonance imaging (MRI)] can be used to model the problem. A detailed discussion of the water heterogeneity also was presented elsewhere.[7] However, the assumption of homogeneous water distribution seems reasonable in our specific application of rat brain studies[8]; therefore our focus is narrowed to the situation with a homogeneous water distribution.

Well-controlled phantom studies were completed to examine the question of whether μ_a and μ_s' could be successfully recovered with our measurements. Starting with the simplest and most predictable model, we examined the performance of our approach in the homogeneous infinite medium. A diffusing phantom with Intralipid and blood in water was used and contained in a cylindrical tank big enough to act as an infinite medium. The absorption was considered as the contribution of water and HbO_2, since enough oxygen was provided. Two 1-mm fibers were used as the source and the detector. The source–detector distance (r) was varied by use of a translation stage with digital readout (accuracy, ~0.1 mm). The multiple-distance method was used to fit the μ_a and μ_s' values at 740 and 840 nm from the measured $A(r)$ and DP(r) curves. The experiment was designed to start with an Intralipid solution with a concentration of 0.5% that was gradually increased to 1.0%, then in the second stage the Intralipid was kept constant and the HbO_2 concentration was increased gradually from 0 to 20 μM. The calculated and the expected values are plotted and compared in Fig. 2. The recovered μ_a agreed within 5% difference (and more consistent to a bias offset) with predicted values from the literature,[9,10] and the recovered μ_s' were within 5% of the expected values[11] if a 12% scaling factor

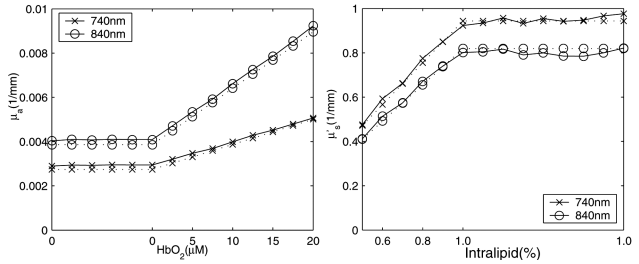

Fig. 2. Predicted (dashed curves) versus reconstructed (solid curves) values for μ_a and μ_s' when both the Intralipid and the HbO_2 concentrations are varied: Left, μ_a versus HbO_2 concentration; right, μ_s' versus Intralipid concentration.

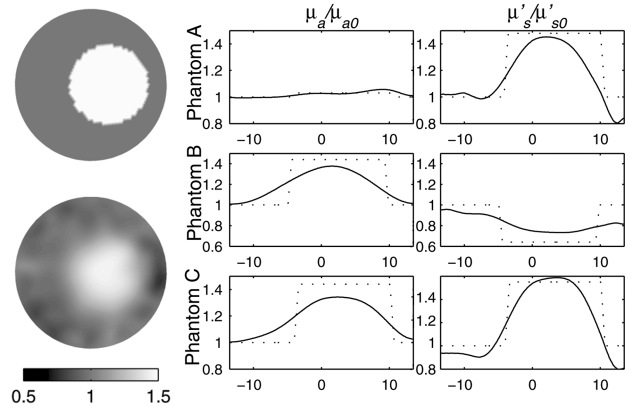

Fig. 3. Left, theoretical desired image with a sample reconstructed set of images. In the cross-section plots (μ_a on the left and μ_s' on the right) are shown for three such phantom tests. Scales are normalized by the background values.

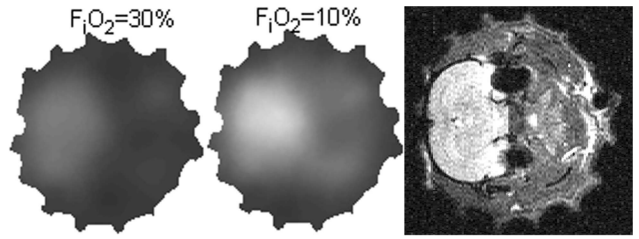

Fig. 4. Examples of reconstructed tomography images of a rat head in normal and hypoxic states are shown. Left, μ_a image (740 nm) at the normal state with the inspired oxygen fraction of 30%. Middle, μ_a of the hypoxic state when the fraction dropped to 10%. The increase in absorption indicated the increased Hb concentration and the decreased saturation. Right, MRI image acquired simultaneously with the NIR measurement, provided the fiber positions for image reconstruction.

was incorporated to account for the Intralipid batch difference. It is important to note that the absolute HbO_2 and Hb content thus can be estimated based on the absorption at 740 and 840 nm.

The significance of our presented method is the application of the multichannel full spectral CCD system in optical tomography studies. To examine further the performance in the typical imaging application, we tested our system on cylindrical phantoms with different absorption or scattering heterogeneities inside. Those phantoms were mixtures of ink, TiO_2, and gelatin with 85% water. Absorption and scattering properties were adjusted by varying the ink or TiO_2 content. A field emission microscopy–based image reconstruction program was used to map the DP to the phase shift in frequency domain. An example of desired images and reconstructed images of a scatter heterogeneity phantom is shown at the left of Fig. 3, and cross-section plots of three representative phantoms are shown at the right. The reconstructed peak values are within 10% of the target values for all cases shown. The method was then applied in a rat cranium imaging study. An example of tomography imaging of the rat head during hypoxia is shown in Fig. 4. The MRI images were acquired, together with the optical measurement to show the location of the brain and fibers in the image. In this case the absorption values in the brain were as expected, and these results represent what is believed to be the first *in vivo* implementation of this technological approach to NIR tomography.

The significance of this work is important for the field of NIR tomography, in that the cost and engineering involved in TDS and FDS system development and calibration is very high. The costs and calibration requirements of second-differential spectral tomography systems may become less as this technology matures, and the present method is clearly simpler than the TDS or FDS approaches. In any case, this report presents what is believed to be the first demonstration of the use of full spectral measurements to image hemoglobin and oxygen hemoglobin in tissue with the second-differential spectral-analysis approach.

This work was sponsored by grants NIH, RO1 NS39471, U54 CA105480, RO1 CA69544, and RO1EB002085. H. Xu's e-mail address is heng.xu@dartmouth.edu.

References

1. S. R. Arridge and W. R. B. Lionheart, Opt. Lett. **23,** 882 (1998).
2. A. Corlu, T. Durduran, R. Choe, M. Schweiger, E. M. C. Hillman, S. R. Arridge, and A. G. Yodh, Opt. Lett. **28,** 2339 (2003).
3. A. Li, Q. Zhang, J. P. Culver, E. L. Miller, and D. A. Boas, Opt. Lett. **29,** 256 (2004).
4. H. Jiang, K. D. Paulsen, U. L. Osterberg, B. W. Pogue, and M. S. Patterson, J. Opt. Soc. Am. A **13,** 253 (1996).
5. S. R. Arridge, M. Cope, and D. T. Delpy, Phys. Med. Biol. **37,** 1531 (1992).
6. S. J. Matcher, M. Cope, and D. T. Delpy, Phys. Med. Biol. **39,** 177 (1994).
7. H. Xu, B. W. Pogue, H. Dehghani, R. Springett, K. D. Paulsen, and J. F. Dunn, Proc. SPIE **4955,** 16 (2003).
8. R. F. Reinoso, B. A. Telfer, and M. Rowland, J. Pharmacol. Toxicol. Methods **38,** 87 (1997).
9. B. L. Horecker, J. Biol. Chem. **148,** 173 (1943).
10. V. Hollis, "Noninvasive monitoring of brain-tissue temperature by near-infrared spectroscopy," Ph.D. dissertation (University College, London, 2002).
11. H. J. van Staveren, C. J. M. Moses, J. van Marle, S. A. Prahl, and M. J. C. van Gemert, Appl. Opt. **30,** 4507 (1991).